ELSEVIER

Journal of Nuclear Materials 313–316 (2003) 1000–1004

journal of nuclear materials

www.elsevier.com/locate/jnucmat

E × B-drift, current, and kinetic effects on divertor plasma profiles during ELMs

T.D. Rognlien [a,*], M. Shimada [b]

[a] Lawrence Livermore National Laboratory, Livermore, CA 94551, USA
[b] ITER International Team, ITER Naka Co-Center, Naka, Ibaraki-ken 311-0193, Japan

Abstract

The transient heat load on divertor surfaces from edge-localized modes (ELMs) in tokamaks can be very large and thus of concern for a large device such as ITER. Models for kinetic modifications to fluid models are discussed that should allow a reasonable description of the long mean-free path regime encountered owing to the high plasma temperatures in the scrape-off layer (SOL) during large ELMs. A set of two-dimensional simulations of the dynamic response of the SOL plasma to an ELM is presented. The role of plasma currents and **E** × **B** motion is emphasized, which cause large changes in divertor density and temperature, but small changes in the outer-plate heat flux.

PACS: 52.40.Hf
Keywords: Divertor plasma modeling; Edge-localized modes (ELMs); 2D edge-plasma transport; **E** × **B** drifts; Plasma edge current

1. Introduction

Edge localized mode (ELM) heat load on material surfaces is a key issue for burning-plasma tokamak experiments, e.g., ITER and FIRE. According to the observations in existing tokamaks, the ELM heat flux on the divertor can have a profile width about twice that of the steady-state heat flux [1]. When the ELM occurs, the plasma with parameters close to those at the top of the so-called pedestal just inside the magnetic separatrix is assumed injected or connected to the open field-line scrape-off layer (SOL). Here, at least two processes occur. One change is the reduction in the plasma pressure gradients, which modifies the bootstrap current, and thus the poloidal magnetic flux surfaces, resulting in a shift of the magnetic separatrix defining the SOL. A second change is flow of the injected plasma to the divertor plates. In this paper, we focus on evaluating the latter process by including the effects of the **E** × **B** drifts and parallel currents, thus extending previous work [2,3] that neglects such effects.

The role of classical **E** × **B**, diamagnetic drifts, and parallel currents in the SOL has been the subject of a number of theoretical and modeling studies, e.g., [4,5], and corresponding experimental measurements [6]. For the high temperatures encountered during and just after an ELM, these effects should be stronger as they increase with temperature. While the ultimate goal is to understand the impact of large ELMs in big devices, in this paper we focus on developing a clear physics picture of present transport models for modest ELMs. Indeed, we find that there is already a rich interaction of processes for this case.

The plan of the paper is as follows: the geometry and model are described in Section 2. Kinetic corrections to the fluid equations are given in Section 3, and time-dependent results for divertor profiles during an ELM are presented in Section 4 followed by a conclusion.

2. Geometry, equations, and ELM model

We use the UEDGE two-dimensional transport code [5] to calculate the plasma and neutral response to an

* Corresponding author. Tel.: +1-925 422 9830; fax: +1-925 423 3484.
E-mail address: trognlien@llnl.gov (T.D. Rognlien).

0022-3115/03/$ - see front matter
PII: S0022-3115(02)01438-1

ELM-like event. To focus on the essential physics, we consider a DIII-D single-null MHD equilibrium with the divertor plates being approximated by surfaces orthogonal to the magnetic flux surfaces. Equations are solved for ion particle continuity and parallel momentum, with the parallel direction being that along the magnetic field, **B**. The current continuity equation is included for the electrostatic potential, ϕ, with ∇B and curvature drifts included and quasineutrality assumed. Separate electron and ion temperature equations are used. The hydrogen neutrals arising from a plate recycling coefficient of $R = 0.99$ are described by a diffusive model, i.e., inertia and viscosity are neglected compared to the strong charge-exchange momentum transfer with ions.

The parallel transport is assumed to be classical [7] with flux-limits on the viscosity, thermal force, heat conductivity terms as discussed in more detail in Section 3. The pre-ELM cross-field transport is assumed to be enhanced over classical values owing to plasmas turbulence; we use a diffusive model here, although convection can also be used. In the pre-ELM state, radial diffusion coefficients used are in the range deduced from present experimental results [1]; for density, $D = 0.25$ m^2/s, for electron and ion energy transport, $\chi_{e,i} = 0.5$ m^2/s; radial ion viscosity for parallel and perpendicular velocities are also set to 0.5 m^2/s. The core-edge ion density is set to 3×10^{19} m^{-3}, and the power into the SOL is 4 MW. At the divertor plates, the poloidal ion velocity, v_{ip}, into the plate is set by the condition $v_{ip} = (\mathbf{E} \times \mathbf{B}/B^2)_p + c_s B_p/B$ [8], where B_p/B is the ratio of the poloidal to total B-field, and c_s is the ion-acoustic speed. The poloidal ion energy flux at the plate is $(5/2)v_{ip} n T_i$, where n is the plasma density, and T_i the ion temperature. The poloidal electron energy flux is $n\bar{v}_e(2T_e + e\phi_s)(B/4B_p)\exp(e\phi_s/T_e)$, where $\bar{v}_e = (8T_e/\pi m_e)^{1/2}$, ϕ_s is electrostatic sheath potential, $-e$ is electron charge, and m_e is electron mass.

The ELM event is modeled by abruptly increasing the diffusion coefficients by a factor of 20 for a time of 200 μs in a broad region around the outer midplane, while the core-edge density and temperatures (~400 eV) are held at their pre-ELM values on the 95% inner poloidal magnetic flux surface as normalized to the separatrix flux. The profile of the enhanced diffusion is a Gaussian shape in the poloidal direction, centered at the outer midplane and having a half-width of 1.9 m. In the radial direction, the enhanced diffusion is uniform to the separatrix and decays exponentially in the SOL with a scale-length of 1 cm.

3. Kinetic extensions for fluid models

The classical parallel transport coefficients given, for example, by Braginskii [7] need to be modified to account for the long mean-free path; here we briefly review and extend those models. Flux-limits restrict the classical diffusive flux to a fraction of the free-steaming flux. For example, the electron thermal flux is limited as follows:

$$q_e = -\kappa_e \frac{\partial T_e}{\partial s_\parallel} \rightarrow -\kappa_e [1 + (q_e/q_f)^2]^{-1/2} \frac{\partial T_e}{\partial s_\parallel}, \quad (1)$$

where T_e is the electron temperature, κ_e is the classical heat conductivity, $s_\parallel$ is the distance along **B**, $q_f = c_e n T_e (2T_e/m_e)^{1/2}$. The coefficient $c_e \approx 0.15$ is obtained by comparisons with Monte Carlo calculations [9]. Similarly, for the ion conduction, $c_i \approx 0.15$, and a corresponding limit for the ion parallel viscosity uses a coefficient of $c_v = 0.5$.

A second correction that must be made is for the thermal force term appearing in the electron parallel momentum equation of the form $0.71 n \nabla_\parallel T_e$. We adjust this term by multiplying it by $1/(1 + \lambda/L_s)$, where L_s is the minimum of the connection length from the midplane to the plate, $L_\parallel$, or the parallel gradient length of T_e, and λ is the mean-free path for Coulomb collisions. The results to be presented here are largely insensitive to this correction.

While details of flux limiting models can be inaccurate [10], we argue that during an ELM event, as the T_e values rise in the SOL, the temperature profile becomes comparatively flat along $s_\parallel$, such that errors in the $T_e(s_\parallel)$ profile are relatively unimportant. The flattening of T_e when it reaches high values near the outer plate is shown in Fig. 1 for the evolution of the poloidal (and thus $s_\parallel$) profile of T_e on a flux surface at 2 mm into the SOL measured at the midplane for the ELM model for the simulation of Section 4. This results in the well-known sheath-limited regime, where the electron energy loss at the divertor can be related to the particle flux Γ_e as

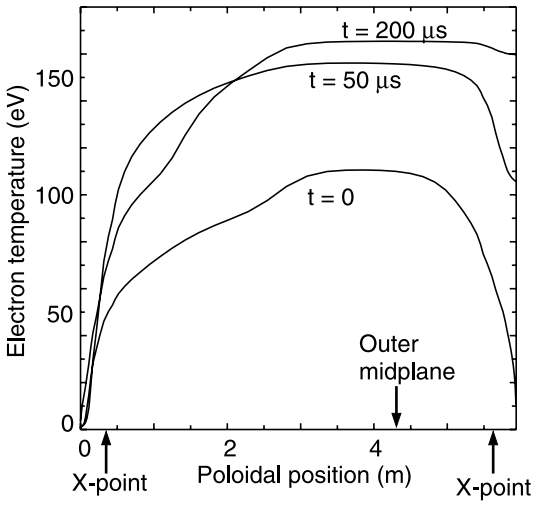

Fig. 1. The poloidal electron temperature profiles for a poloidal flux surface 2 mm outside the separatrix at the midplane at three times following an increase of the anomalous diffusion coefficients by a factor of 20.

$$(2\beta T_e + e\phi_s)\Gamma_e = (2\beta T_e + e\phi_s)n(\bar{v}_e/4)\exp(e\phi_s/T_e). \quad (2)$$

Owing the exponential dependence, the most important factor setting Γ_e is the sheath potential, and $\beta = 1$.

The model of the sheath-limited regime can be extended to very long mean-free paths where the electron distribution function can become depleted in velocity space corresponding to the velocity region where single-transit escape is possible. Then velocity scattering into this region determines the electron loss rate. The loss rate for the transition from the sheath-limited regime to this velocity-space regime has been considered previously [12], and shows that the electron particle flux escaping at the plate can be well approximated as

$$\Gamma_e \to \frac{n\bar{v}_e \exp(e\phi_s/T_e)}{4(1+\tau_p/\tau_c)}. \quad (3)$$

Here τ_p is long mean-free path confinement time [11], and τ_c is the confinement time for the collisional sheath-limited case [12]. In Eq. (3), the factor $\zeta \equiv 1/(1+\tau_p/\tau_c) \approx 1/[1+\alpha_c(\lambda/L_\parallel)(e\phi_s/T_e)]$ with $\alpha_c \approx 0.5$ gives a smooth transition to the regime where electron loss is set by velocity-space diffusion from Coulomb collisions when $\tau_p > \tau_c$ [12]. Also, when $\tau_p > \tau_c$, $\beta \to 0.5$. The ions are not confined, so they flow out owing to their thermal velocity and the 'ambipolar' electric field; however, reversal of the outward flow can arise from $\mathbf{E}\times\mathbf{B}$ and local source effects.

The sheath potential can thus be calculated that includes both short and long mean-free path regimes. The current through the sheath, J, must be the sum of the ion and electron contributions;

$$J = nec_s + nev_{\perp e}B/B_p - ne\zeta(\bar{v}_e/4)\exp(e\phi_s/T_e), \quad (4)$$

where the typically small second term arises from detailed consideration of the $\mathbf{E}\times\mathbf{B}$ and diamagnetic electron velocity, $v_{\perp e}$, at the plate [8]. Inverting this equation gives the sheath potential as

$$-\frac{e\phi_s}{T_e} = \ln\left(\frac{\zeta\bar{v}_e/4\hat{c}_s}{1-J/J_{sat}}\right), \quad (5)$$

where $\hat{c}_s \equiv c_s + v_{\perp e}B/B_p$, and $J_{sat} = ne\hat{c}_s$ is the ion saturation current. Note that ζ also depends on ϕ_s, but unless the edge temperature is very high, $\zeta \approx 1$. For $\zeta = 1$ and $J = 0$, Eq. (5) gives the familiar results of $e\phi_s/T_e \sim 3$ for deuterium. For the ELM simulations in the next section, we find regions where $J \sim J_{sat}$, which strongly affects ϕ_s.

4. Transport simulations during a simulated ELM

As mention in Section 2, the ELM is simulated by increasing the diffusion coefficients by a factor of 20 over a broad area encompassing the outer midplane for 200 μs. The response of T_e in the SOL can be seen in Fig. 1. Owing to the low T_e conditions at the inner plate, much of the T_e rise occurs at the outer plate in the first 50 μs; the inner leg temperature rises more slowly because electron convection (a current) carries most of the energy to the outer plate and because the plasma density is higher on the inner-divertor leg.

The impact of including, or not, the cross-field drifts ($\mathbf{E}\times\mathbf{B}$ and diamagnetic) and current is illustrated for the plasma density at the outer plate in Fig. 2. The three major peaks shown late in the ELM injection for no current or drifts is a complicated interplay of the time response to strong heat pulse from the ELM and the recycling neutrals, leading to regions of local poloidal flow reversal. We have verified that the structure is not a numerical artifact by performing mesh resolution studies. Rather than focusing on this density structure, one should note from Fig. 2 that with drifts and current, the multiple peaks largely disappear. Also, the density decreases substantially from the pre-ELM state. The reason for the density decrease is large $\mathbf{E}\times\mathbf{B}$ poloidal flow reversal, as will be illustrated shortly. Note that the pre-ELM density is shifted to the left for the lower figure with $\mathbf{E}\times\mathbf{B}$. This shift is explained by the radial $\mathbf{E}\times\mathbf{B}$ drift near the plate; i.e., the direction of $\mathbf{B}$ is dominantly out of the plane of Fig. 2 (ion $\nabla\mathbf{B}$ is downward), such that the normal downward poloidal electric field produces a drift of ions and electrons to the left, toward the private flux region.

A primary quantity of interest is the integrated energy deposited on the plates during the ELM injection.

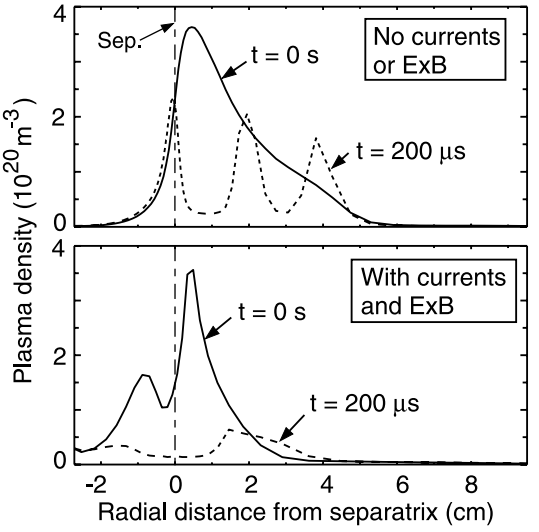

Fig. 2. Plasma density profiles on the outer plate for two times in the ELM simulation for cases with no cross-field drifts and current, and then with drifts and current.

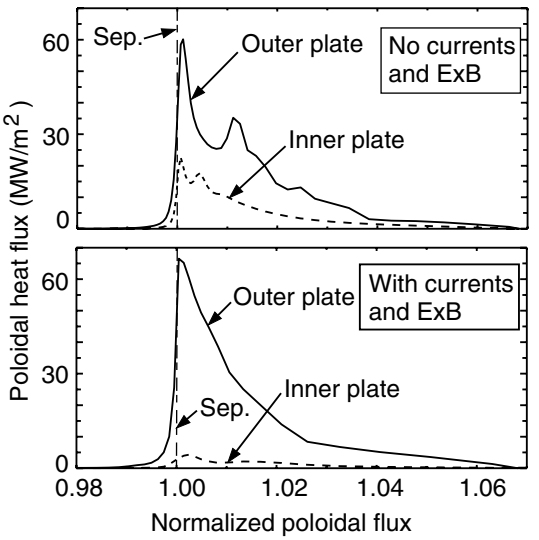

Fig. 3. Time-averaged energy density deposited on the divertor plates for $t = 0$–200 μs duration of the ELM. About 50% of the 6 kJ injected during the 200 μs period arrives in this time interval.

The energy flux during the enhanced-diffusion ELM state ($t = 0$–200 μs) is compared in Fig. 3 for the cases with, and without, drifts and currents. The energy flux is plotted versus poloidal flux, with unity corresponding to the separatrix. The energy flux is much smoother versus radius than the density profile from Fig. 2 for two reasons: the T_e profile (not shown) has minima where n_i has maxima, and the energy fluxes are averaged over 200 μs. The case with drifts shows very little fine structure, again in part from the T_e variation, but also from the dominating electron current which convects energy to the outer plate over most of the poloidal extent of the SOL. Also note that the heat flux to the inner plate is significantly reduced when current and drifts are allowed. The ELM pulse injects about 6 kJ into the SOL, with about 1/2 of it appearing during the 200 μs period in Fig. 3, and the majority of the remainder appearing in the second 200 μs period when the diffusion is returned to low initial values. The effect of the drifts and current is to delay the deposition time by ~20%.

The effect of the $\mathbf{E} \times \mathbf{B}$ drifts on outer plate density during the ELM pulse can be understood from the vector plot of the ion flux × area shown in Fig. 4 at two times: (a), $t = 0$ s and (b), $t = 27$ μs. Initially, most of the ion flux is directed toward the plate, although there is a large flow in the private-flux region from the outer divertor to the inner divertor, as reported elsewhere. After the ELM pulse, the rapid rise in T_e and ϕ gives a stronger $\mathbf{E} \times \mathbf{B}$ poloidal flow, causing flow reversal, i.e., ion flow up along both sides of the separatrix; this flow depletes the density near the plate, yielding the large drop seen in Fig. 2.

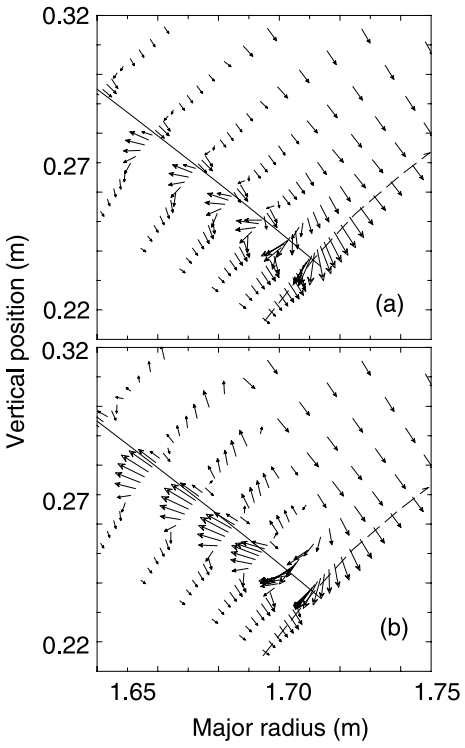

Fig. 4. Vectors of ion plasma particle flux × area near the outer separatrix for (a), $t = 0$ μs and (b), $t = 27$ μs with cross-field drifts and current on. The solid and dotted lines are the magnetic separatrix and divertor plate, respectively.

Finally, the effect of the parallel current is illustrated by considering the parameter $e\phi_s/T_e$ as given in Eq. (5) at each plate for two different times during the ELM simulation in Fig. 5. The current flows from the outer plate (high T_e) to the inner plate (low T_e) through the plasma. There is an electrical current initially ($t = 0$ s), it being directed away from the outer plate outside the separatrix (excess electrons flowing into the plate). This current is small compared to the saturation current, yielding an initial ratio $e\phi_s/T_e$ is close to its zero-current value of ~3 for deuterium. However, during the ELM pulse ($t = 200$ μs), these values change dramatically, as shown in the lower frame in Fig. 5. During this period, the magnitude and the width of the current increase, and the associated convected electron power to the outer dominates conduction by a factor of ~5. At the inner plate, most electrons are reflected so that the ions can carry the required current through the sheath, and at the outer plate, the low $e\phi_s/T_e$ is needed to allow sufficient electrons to carry the current through the sheath, both because the current is larger and the plasma density at the plate is lower. The different values of $e\phi_s/T_e$ have important consequence for the ion energy spectrum reaching the plate surface, since each ion acquires the

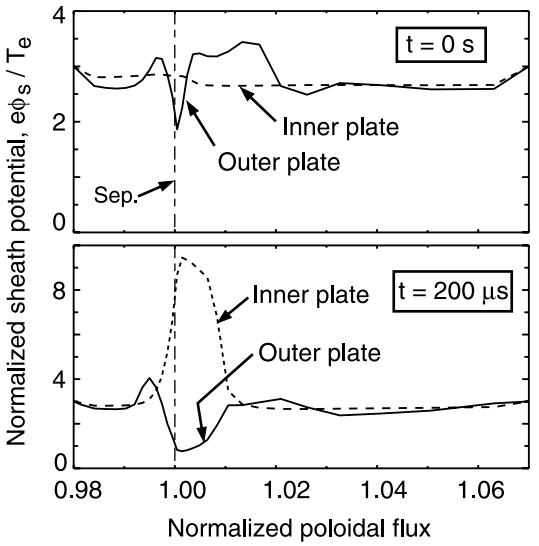

Fig. 5. Calculated $e\phi_s/T_e$ profiles at the inner and outer divertor plates at two times with cross-field drifts and current on. Peak outer plate $T_e \approx 170$ eV, while on the inner plate, $T_e \approx 5$ eV.

sheath potential in transiting to the plates. The sheath potentials themselves have broad maxima of ~50 and ~200 V at the inner and outer plates, respectively.

5. Conclusions

It is argued that kinetic corrections to fluids equations allow one to use fluid transport codes to investigate the SOL response to ELMs. The model of the electron confinement by the sheath potential is extended to the very long mean-free path regimes. Simulation of a modest ELM shows that the cross-field drifts and plasma current can have large effects on the divertor plasma density, temperature, and sheath potential. $\mathbf{E} \times \mathbf{B}$ drifts cause a radial shifting and poloidal flow reversal. However, the integrated heat flux profile to the outer divertor is changed little; the inner divertor receives substantially less energy when the drifts and currents are present owing to a strong convection of electron energy toward the outer plate. These results show the strong role that electron energy convection via parallel current can play. Thus, mechanisms that control the direction of this current, including non-axisymmetric effects, are likely important for understanding ELM energy deposition. For example, changing the direction of the toroidal B-field often changes the direction of the parallel current in our simulations. The present calculations also need to be extended to higher ELM energy.

Acknowledgements

This work was performed under the auspices of the US Department of Energy by the University of California Lawrence Livermore National Laboratory under contract no. W-7405-Eng-48.

References

[1] R. Stambaugh et al., ITER Physics Basis, Nucl. Fusion 39 (1999) 2391 (Chapter 4).
[2] R. Schneider et al., Fusion Energy 1996, Proceedings of 16th International Conference, Montreal, 1996, vol. 2, IAEA, Vienna, 1997, p. 465.
[3] T.D. Rognlien, J.A. Crotinger, et al., J. Nucl. Mater. 241–243 (1997) 590.
[4] A.V. Chankin, J. Nucl. Mater. 241–243 (1997) 199.
[5] T.D. Rognlien, D.D. Ryutov, N. Mattor, G.D. Porter, Phys. Plasma 6 (1999) 1851.
[6] M.J. Schaffer et al., Phys. Plasma 8 (2001) 2118.
[7] S.I. Braginskii, in: M.A. Leontovich (Ed.), Transport processes in a plasma, Reviews of Plasma Physics, vol. 1, Consultants Bureau, New York, 1965, p. 205.
[8] R.H. Cohen, D.D. Ryutov, Comm. Plasma Phys. Contribution Fusion 16 (1995) 255;
Phys. Plasmas 2 (1995) 2011.
[9] R.H. Cohen, T.D. Rognlien, Contribution Plasma Phys. 34 (1994) 198.
[10] O. Batishchev et al., Phys. Plasma 4 (1997) 1672.
[11] V.P. Pastukhov, Nucl. Fusion 14 (1973) 3.
[12] T.D. Rognlien, T.A. Cutler, Nucl. Fusion 20 (1980) 1003.